Available online at www.sciencedirect.com
SCIENCE DIRECT®
Journal of Nuclear Materials 334 (2004) 189–194
journal of nuclear materials
www.elsevier.com/locate/jnucmat

Carbothermic reduction of uranium oxides into solvent metallic baths

Thomaz A. Guisard Restivo [a,*], José D.T. Capocchi [b]

[a] Laboratório de Materials Nucleares, CTMSP, Rod. Sorocaba-Iperó km 12,5, 18560-000 Iperó SP, Brazil
[b] Escola Politécnica da USP, Dpto Metalurgia e Materiais, Av., Prof. Mello Moraes 2463, 05508-900 São Paulo SP, Brazil

Received 15 December 2003; accepted 23 June 2004

Abstract

The carbothermic reduction of UO_2 and U_3O_8 is studied employing tin and silicon solvent metallic baths in thermal analysis equipment, under Ar inert and N_2 reactive atmospheres. The metallic solvents are expected to lower the U activity by several orders of magnitude owing to strong interactions among the metals. The reduction products are composed of the solvent metal matrix and intermetallic U compounds. Silicon is more effective in driving the reduction since there is no residual UO_2 after the reaction. The gaseous product detected by mass spectrometer (MS) during the reduction is CO. A kinetic study for the Si case was accomplished by the stepwise isothermal analysis (SAI) method, leading to the identification of the controlling mechanisms as chemical reaction at the surface and nucleation, for UO_2 and U_3O_8 charges, respectively. One example for another system containing Al_2O_3 is also shown.

1. Introduction

The carbothermic reduction is the most desirable process for recovering metals from oxides and ores owing to the low cost and availability of carbon. Normally the metal oxides undergoing reduction should be less stable than CO according to thermodynamics, while the metal must be a weak carbide former. These characteristics are not found in reactive metal oxides, including uranium. The successful carbothermic reduction of such oxides can still be done by means of some thermodynamic skill [1,2]. The general carbothermic reduction equation can be written:

$$M_xO_y(s) + yC(s) = xM + yCO(g). \quad (1)$$

The carbide forming reaction must be avoided:

$$mM + nC(s) = M_mC_n. \quad (2)$$

Both reactions can be shifted to the required directions by lowering the metal activity a_M, while the condition can be expressed by:

$a_{M(1)} < a_{M(2)}$; $a_{M(2)}$ required for accomplishing the carbide forming reaction.

The activity is decreased by solving the reduced metal into a metallic bath as soon as it is formed. Once the metallic solvent bath shows strong attraction to the reduced metal, it is expected that the metal activity will then be several orders of magnitude smaller than a

* Corresponding author. Fax: +55 15 229 8460.
E-mail address: guisard@dglnet.com.br (T.A. Guisard Restivo).

0022-3115/$ - see front matter © 2004 Elsevier B.V. All rights reserved.
doi:10.1016/j.jnucmat.2004.06.006

simple mixing law. One can anticipate the lowering effect on the reduced metal activity by examining the binary phase diagram: the presence of high melting point intermetalics indicates a strong interaction between the metals, prevailing even after complete melting of the system [3]. One further technique to drive reaction (1) is to lower the actual P_{CO} during the process below equilibrium values by evacuating the system or by flowing inert gas.

However, if these modified thermodynamic conditions are not enough to drive the reduction reaction forward to the metal product, then there is a third technique that may be employed for nitride-forming reactive metals. It consists of replacing the inert gas or vacuum by nitrogen gas [1,2,4]. The so called carbonitrothermic reduction method is based on the large negative free energy for the nitride forming reaction.

$$\underline{M}_{Msolv} + 1/2\,N_2 = MN(s), \tag{3}$$

$$M_xO_y(s) + yC(s) + zN_2(g) = M_xN_{z/2}(s) + yCO. \tag{4}$$

Reaction (4) is the coupled result from reactions (1) and (3) and does not depend on reduced metal activity. Therefore, high conversion is expected by using the carbonitrothermic reduction.

The work presents some results on reduction of uranium oxides by carbon in tin and silicon metallic baths, carried on thermoanalytical instruments. While the Sn bath was used for an explorative study, where some basic process data were determined, the Si bath was investigated on a more detailed basis, including a kinetic investigation.

2. Experimental

Thermoanalytical equipment was employed on the main part of the work, composed by a simultaneous TGA/DTA coupled with mass spectrometer (MS). The crucibles were made of graphite and alumina, filled with the reaction mixtures weighed near 300 mg. The TGA/DTA support was built in WRe alloys, rather resistant to metal vapors at high temperatures. The heating rates established were either 10 °C/min or 15 °C/min, until the high temperature isotherm (1550–1670 °C), afterwards following the cooling curve at 15 °C/min, allowing to register the exothermic peaks related to the alloy solidification. The atmospheres were dynamic flowing high purity Ar and N_2 (99.999%) rated at 150 ml/min.

All the reagents were in powder form. The UO_2 powder used in the first part of the exploratory study was reduced from AUC in a fluidized bed reactor, resulting in high specific surface area (BET = 5.61 m^2/g) and mean particle size 7.6 μm. The O/U ratio measured was 2.24. For the second part-detailed study under Si bath–the UO_2 powder had the same characteristics, except for a lower O/U ratio: 2.10. Both powders were nuclear grade, with impurities content less than 200 ppm. Tin powder was reagent grade (+99.9%) and Si powder purity was 99+%. Two kind of carbon source were used: graphite electrode-grade and carbon black, mainly differing on surface areas, 0.5 and 51 m^2/g respectively. The mixing of the powders were accomplished at a Turbula mixer for 3 h. Some pellets pressed at 200 MPa were prepared from the mixture in order to increase the reagent contacts prior to the reaction.

3. Results and discussion

3.1. Exploratory study

One typical reduction curve is shown in Fig. 1 for graphite reducer into Sn bath. The first mass loss is ascribed to the initial reduction $UO_{2.24}$ to $UO_{2.00}$, due to carbon. The Sn melting and alloy solidification were registered, besides the mass loss due to CO evolution. The results compilation can be seen in Fig. 2 for the Sn bath, scaled to temperature, whereas the experimental conditions were varied: soaking times, temperatures, and sample characteristics. The reduction conversion was assumed to be measured by the total mass loss on each condition. It can be concluded the carbon black (also called amorphous carbon, Cam) yields a greater mass loss, meaning the reduction was favoured. Excess carbon over the stoichiometric amount resulted in smaller conversion. This effect, not fully understood, seems to be related to the less effective contact patterns and decreasing fluidity of the mixture since there is less molten phase. By comparison between curves at different isotherms, there is some evidence that higher temperatures lead to greater conversions. Fig. 3 holds the results

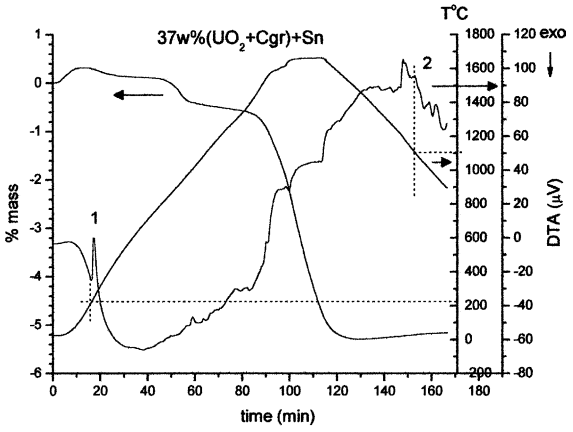

Fig. 1. TGA/DTA analysis for carbothermal (graphite) reduction of UO_2 under Sn bath. 1: Sn melting; 2: alloy solidification.

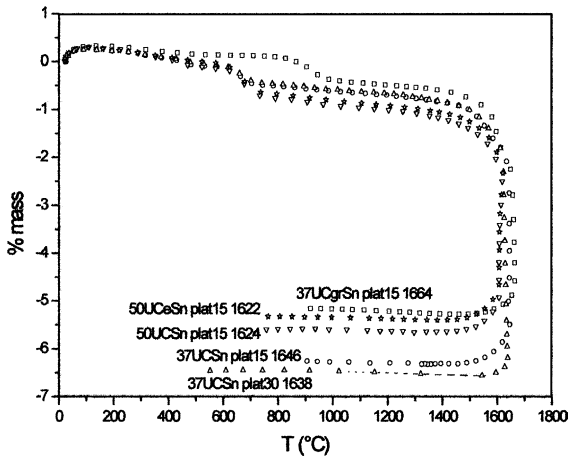

Fig. 2. UO_2 carbothermic reduction under Sn–results compilation, heating rate 10 °C/min. 37UCgrSnplatl5 1664: 37 wt%(UO_2 + Cgr) + Sn, 15 min high temperature plateau, plateau temperature 1664 °C; 50UCeSnplatl5 1622: 50 wt%(UO_2 + Cam(50 wt% in excess)) + Sn, 15 min plateau, plateau temperature 1622; 37UCSn plat30 1638: 37 wt%(UO2 + Cam) + Sn, 30 min plateau, plateau temperature 1638 °C.

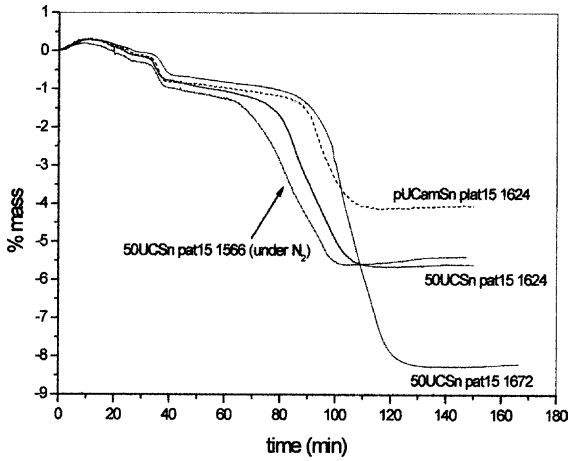

Fig. 3. TGA/DTA carbothermic reduction results scaled to time; heating rate 15 °C/min. The sample codes are the same as previous; pUCamSn Plat 15 1624: refer to a pelletized mixture (UO_2 + C) inside the Sn powder; 50UCSn pat15 1624: actual heating rate 20 °C/min.

scaled to time allowing to more ascertains on the basic process parameters and methods. Time scaling allows a more detailed view on the total mass loss differences. It was found the N_2 reactive atmosphere shifts the reduction reaction to lower temperatures maintaining the same yield. The higher final isotherm temperature has a beneficial effect, while the charge pelletizing (UO_2 + C mixture) is detrimental.

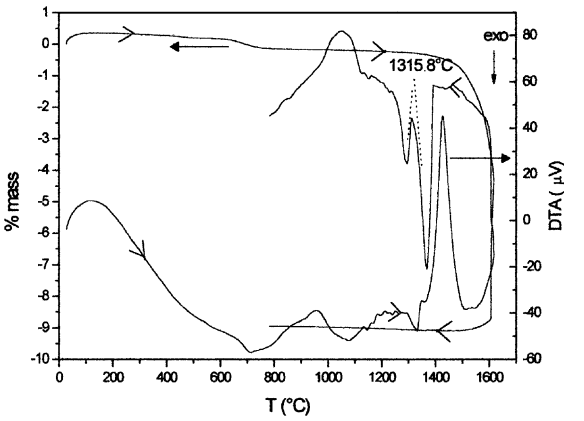

Fig. 4. UO_2 Carbothermic reduction under Si bath. Eutectic solidification at 1315.8 °C.

The silicon solvent bath was tried since the phase diagram U–Si shows high melting point intermetallic compounds. The appeal from dispersion fuel alloys preparation was also considered, since the present process could be extended to alloy production. The reduction under Si bath is presented in Fig. 4. Silicon melting and alloy solidification can be noted. The eutectic sequence has a exact concordance with the 1315 °C eutectic temperature from phase diagram. The reduction rate is also greatly increased when the Si bath is employed compared to Sn bath, demonstrating Si is more effective to drive the reduction to the products side and so to lower the U activity.

The alloys were prepared for metalographic analysis, where the resulting SEM features are shown in Fig. 5. Qualitative analysis by EDS and X-ray diffraction have found the compounds USn_3, UC, UC_2 and residual UO_2 for the process using Sn baths. For the Si case, there was no residual UO_2 and no uranium carbides, meaning the process exhibits high conversion.

3.2. Carbothermic reduction in Si baths

In opposition to the Sn containing charge, the UO_2 + C + Si is a complicated system since all components react with each other. Thermodynamics calculations show that U and Si carbides are the most stable phases and therefore U would be released to the alloy only if its activity is greatly reduced. Fig. 6 shows the TGA/DTA/MS reduction analysis with Si bath for a target alloy 70 wt% Si–30 wt% U. The reduction starts slowly at about 1200 °C, accelerating after Si melting where the main gaseous product is CO. One can verify the eutectic solidification on cooling. The postulated reaction mechanism begins with the C dissolution in Si and competitive reduction of UO_2 by C and Si,

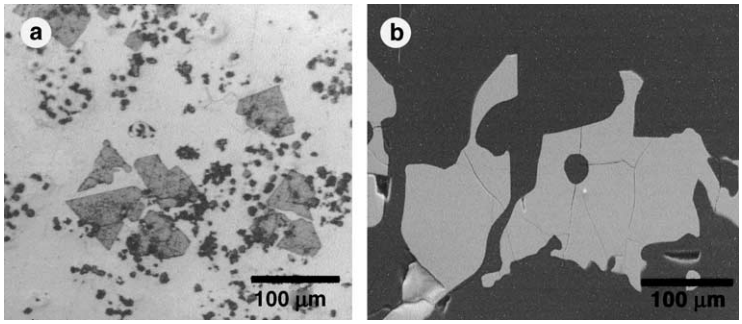

Fig. 5. SEM micrographies, (a) reduction under Sn; (b) reduction under Si.

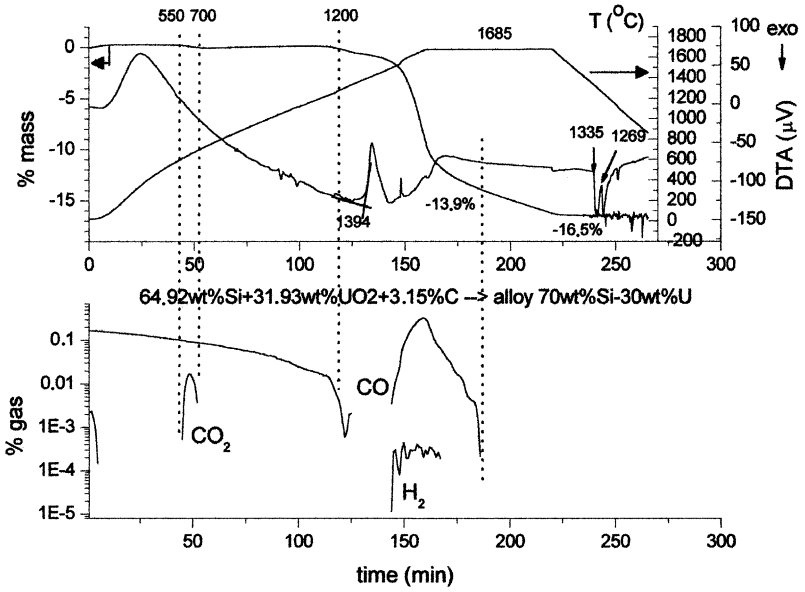

Fig. 6. TGA/DTA/MS analysis for carbothermic reduction in a Si bath.

since there is some evidence on SiO formation. The alloy formed is composed by a pure Si matrix and intermetallic USi_3, according to semi-quantitative EDS analysis. X-ray diffraction revealed the mentioned phases and also a small SiC amount. The last was not recognised as a constituent by SEM/EDS, being ascribed to localised reaction Si–C from the crucible material. When the whole charge was pressed (i.e., 100 MPa, uniaxial press) an improvement on the reduction was achieved. In this case it was found, based on CO release, that the reduction takes place earlier, as well as the resulted alloy shows higher uranium content. There is some evidence that either Si–UO_2 or Si–C reactions are favoured by approaching the particles by pressing. It must be mentioned the U_3O_8 reduction by C into Si bath gave the same products and similar alloys.

3.3. Kinetic analysis

The carbothermic reduction of UO_2 into Si bath was studied by SIA method [5–7], which has being applied successfully by the author for ceramic sintering kinetics [8–10]. The SIA technique is accomplished by limiting the reaction rate between two limits.

During the normal heating, when the reaction rate given by dm/dt reaches one given upper limit, the thermobalance starts an isotherm until a chosen minimum dm/dt value is attained, when the heating is resumed. This process continues up to the final programmed plateau, leading to a heating profile made up of several isotherms, wherein the kinetic models are applied (Fig. 7). The control can be exerted by the sample itself or commanded by the operator, in that case called 'forced SIA' (FSIA). The last type was employed in the present study.

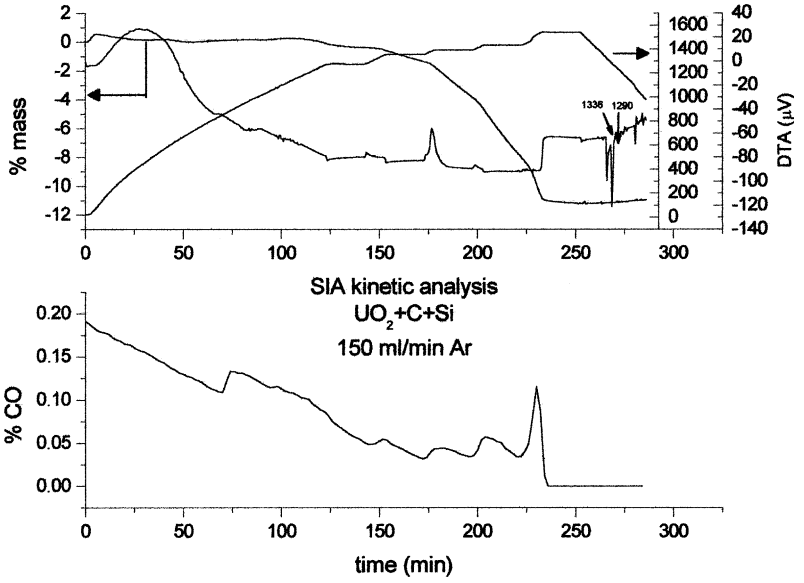

Fig. 7. SIA kinetic analysis on UO_2 reduction.

Both the differential and integral data treatment methods were performed [11,12]:

(a) Differential method: $$d\alpha/dt = k.f(\alpha), \quad (5)$$

(b) Integral method: $$g(\alpha) = k.t. \quad (6)$$

The conversion factor α is given by:

$$\alpha = -(m_{UO2i} - m_{UO2t})/m_{UO2i} = -0.173\Delta m. \quad (7)$$

where $m_{UO2i,t}$ is the initial (at the time t) oxide mass, Δm is the mass loss measured which corresponds to the CO mass released from the reduction reaction. The rate constant k obeys the Arrhenius equation:

$$k = A\exp(-Ea/RT). \quad (8)$$

The graphic $\ln k \times 1/T$ has a slope $-Ea/R$, where Ea is the activation energy.

The data treatment should be based on several rate equations known in the literature. Though the normal procedure is to test all the equations, the present work considered the Sestak–Berggren equation which could hold most part of the proposed models [13]:

$$d\alpha/dt = k \cdot \alpha^m \cdot (1-\alpha)^n \cdot [-\ln(1-\alpha)]^p. \quad (9)$$

The method applied the expression (5) and (6) to the thermogravimetric data for each term of Eq. (9) as the α function, to search which one shows the best linear fit. The functions $f(\alpha) = \alpha^m$ and $f(\alpha) = (1-\alpha)^n$ fit better, while only $f(\alpha) = (1-\alpha)^n$ gave a good Arrhenius plot (Fig. 8). The result suggests the reduction is controlled by chemical reaction at the UO_2–Si interface, with a reaction order in the range 0.3–0.4 and activation energy

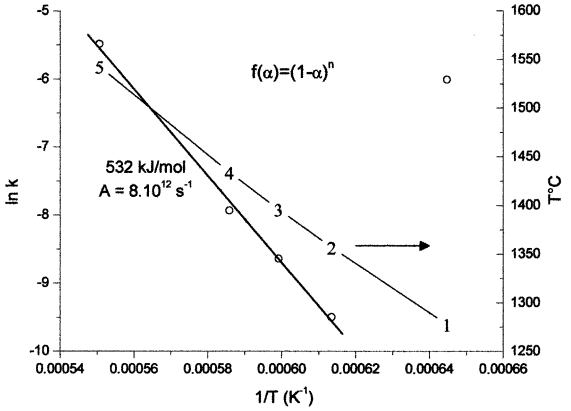

Fig. 8. Arrhenius plot for $f(\alpha) = (1-\alpha)^n$; activation energy 532 kJ/mol.

532 kJ/mol. A lower value of activation energy (163 kJ/mol) was obtained by calculating alpha from the CO gas amount evolution detected on MS during reaction. This was probably due to the delay on the gas signal response from the crucible to the quadripole sensor. One should consider the delay into its most general meaning, say, the time spent by highly diluted CO molecules in argon flow to percolate into the capillary tube and reach its minimum detectable content at the quadripole, or even the interaction between CO and SiO (Si) vapors at a given transitory condition, leading to composition changes. Actually, several experiments have shown an increase on the CO content according to MS during the isotherms, not matching the plateau limits.

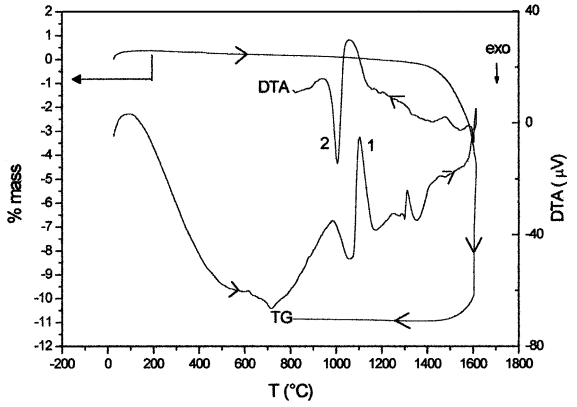

Fig. 9. TGA/DTA analysis on the carbothermic reduction of Al_2O_3 melting; 2: alloy solidification.

The U_3O_8 reduction case presented a totally different behaviour, giving no good fitting to the Eq. (9) terms and even for other traditional rate equations. The only equation fitting linearly the thermogravimetric data was the so called Johnson–Mehl equation (J–M), in the differential form:

$$\frac{d\alpha}{dt} = k^n \cdot t^{n-1} \cdot (1-\alpha), \quad t = \text{time in seconds} \tag{10}$$

$$\int \frac{d\alpha}{1-\alpha} = \int k^n \cdot t^{n-1}\, dt \quad \Rightarrow -\ln(1-\alpha) = k^n \cdot t^n/n$$
$$\Rightarrow \ln\ln(1/(1-\alpha)) = n\ln k + n\ln t - \ln n \tag{11}$$

Applying Eq. (11) on the thermogravimetric data resulted on linear plots during the isotherms. Equation J–M has been used in the FeO reduction into Fe-C saturated bath [14], similar to the present case, and indicates nucleation control. The activation energy determined in this case, in the range 15–40 kJ/mol, gives more evidence on nucleation mechanism. The results suggest some carbides are being formed before U solving into Si. Due to the large particle contraction at the initial reduction $U_3O_8 \rightarrow UO_2$, the contact Si–UO_2 may not be available and carbide formation favoured. Since carbides are unstable into the bath, the reduction follows until U solving and alloy formation.

3.4. Further systems

Other systems were studied using the same experimental approaches: ZrO_2 + C + Cu and Al_2O_3 + C + Cu. Zirconium containing system has produced ZrC, meaning the thermodynamic conditions are not enough for the complete reduction. But alumina was totally reduced by carbon in a copper bath. Fig. 9 shows the TGA/DTA curve for the reduction where the alloy formed consists of Cu matrix and Al in solid solution. According to X-ray analysis, the Cu peaks are strongly shifted from the pure Cu profile, indicating the Al is present.

4. Conclusions

Carbothermic reduction of reactive metals into solvent metallic baths is a promised technically feasible process. Uranium oxides are reduced into Sn and Si bath, the last being more effective to drive the reduction. The products obtained in the reduction were alloys composed by the solvent metal matrix and the intermetallics USn_3 and USi_3. The kinetic evaluation on the reduction demonstrate the controlled mechanism is chemical reaction at the interface for UO_2 reduction case, while changed for nucleation control for U_3O_8.

References

[1] R.N. Anderson, N.A.D. Parlee, J. Vac. Sci. Technol. 13 (1) (1976) 526.
[2] R.N. Anderson, N.A.D. Parlee, Carbothermic method for converting a reactive metal oxide to metal or nitride form in a specific moten metal solvent. UK Patent 1, 342,991, 18 January 1971.
[3] R.N. Anderson, N.A.D. Parlee, Metall. Trans. 2 (1971) 1599.
[4] R.N. Anderson, N.A.D. Parlee, J.M. Gallagher, Nucl. Technol. 13 (1972) 29.
[5] O.T. Sorensen, Thermochim. Acta 50 (1981) 163.
[6] O.T. Sorensen, J. Therm. Anal. 38 (1992) 213.
[7] P.L. Husum, O.T. Sorensen, Thermochim. Acta 114 (1987) 131.
[8] C.C. Guedes e Silva, T.A.G. Restivo, Estudo dos mecanismos de difusão em cerâmicas a base de alumina. in: 14° Congresso Brasileiro de Ciência e Engenharia de Materiais, Águas de São Pedro: CBECIMAT, 2000, Proceedings, TC102-009.
[9] T.A.G. Restivo, L. Pagano Jr., Sintering studies on the $UO_2 \cdot Gd_2O_3$ system using SID method, in: Conference on Characterization and Quality Control of Nuclear Fuels 2002, IAEA, Hyderabad, India, 2003, Proceedings.
[10] T.A.G. Restivo et al., Effect of additives on the sintering kinetics of the $UO_2 \cdot Gd_2O_3$ system, in: TCM Brussels, October 2003, Proceedings.
[11] F. Chen, O.T. Sorensen et al., J. Ther. Anal. 53 (1998) 397.
[12] O. Levenspiel, Engenharia das Reações Químicas, vol. 2. Cálculo de Reatores, John Wiley, EUA, 1972.
[13] M.E. Brown, et al., Thermochim. Acta 355 (2000) 125.
[14] P. Basu, H.S. Ray, J. Therm. Anal. 45 (1995) 1533.